CHEMISTRY
A EUROPEAN JOURNAL

DOI: 10.1002/chem.200700574

Acetonitrile-Facilitated Reductive Dimerization of TCNE to Octacyanobutanediide, $[C_4(CN)_8]^{2-}$, by Iron(II) Chloride

Konstantin I. Pokhodnya,[a] Michael Bonner,[a] Antonio G. DiPasquale,[b] Arnold L. Rheingold,[b] and Joel S. Miller*[a]

Abstract: The redox properties of MCl_2 (M = Mn, Fe, Co) acetonitrile solvates were electrochemically and spectroscopically characterized. The three voltammogram waves at 0.86, 0.48, and 0.21 V versus SCE for $FeCl_2$ dissolved in MeCN are assigned as one-electron reduction potentials for $[Fe^{II}Cl_x(NCMe)_{4-x}]^{2-x}$ ($1 \leq x \leq 3$), respectively, and only $[Fe^{II}Cl_3(NCMe)]^-$ {and $[Fe^{II}Cl_4]^{2-}$ ($E^{\circ}_{1/2} = 0.04$ V vs. SCE), if present} has a potential sufficient for TCNE reduction. The presence in solution of $[Fe^{II}(NCMe)_6]^{2+}$ was also spectroscopically confirmed. The reduction potentials of $M^{II}Cl_2$ (M = Mn, Co) acetonitrile adducts were inadequate to reduce TCNE. $FeCl_2$ reacts with TCNE in MeCN to form $[Fe^{II}\{C_4(CN)_8\}(NCMe)_2]$ (**4**), which is composed of layers of octahedral Fe^{II} ions equatorially bonded to the four terminal N atoms of the μ_4-$[C_4(CN)_8]^{2-}$ ion, with *trans*-MeCN groups and with 15-membered rings. Formation of **4** requires the simultaneous presence of $[TCNE]^{\bullet -}$ and $[Fe^{II}(NCMe)_6]^{2+}$ in solution, which is in contrast to when $[(NEt_4)_2][Fe^{II}Cl_4]$ was used to reduce TCNE. A reaction scheme is proposed. Paramagnetic $[Fe^{II}\{C_4(CN)_8\}(NCMe)_2]$ exhibits substantial antiferromagnetic coupling ($\theta = -13.3$ K), and orders as an antiferromagnet below 7.8 K. The irreversibility of zero-field and field-cooled magnetization suggests that the material exists below T_c in two magnetic states relatively close in energy, that is, the purely antiferromagnetic ground state and a slightly canted antiferromagnetic metastable state.

Keywords: acetonitrile · cyanocarbon · electrochemistry · iron · magnetic properties

Introduction

Magnetic materials are indispensable in a modern society, and the search for advanced magnets remains in the focus of the contemporary materials science.[1] Molecule-based magnets are a relatively new class of magnetic materials in which inorganic or/and organic ions or molecules bearing unpaired electron-spin density strongly interact magnetically through bonds or/and space.[2] $[M^{II}(TCNE)_x]$ (M = V, Mn, Fe, Co, Ni; TCNE = tetracyanoethylene; $x \approx 2$) organic-based magnets have magnetic ordering temperatures (T_c) that range from 44 (M = Co, Ni)[3] up to ≈400 K for M = V.[4,5] In addition, $[V(TCNE)_x]$ is a magnetic semiconductor with a room temperature conductivity of $\approx 10^{-3}$ S cm^{-1}, and spin-polarized electrons in valence and conducting bands that suggest spin-dependent transport applications.[6,7]

$[M^{II}(TCNE)_2]$ (M = Fe, Mn, Co, Ni) magnets can be prepared from the reaction of the anhydrous M^{II} iodide, used in the form of the MeCN solvate, and TCNE in CH_2Cl_2.[3] Compounds of $[M(NCMe)_6][MI_4]$ (M = Fe, Mn) composition were isolated from the corresponding solvate;[8] however, in solution solvates exist in equilibrium between MeCN and I^- ligands coordinated to the M^{2+} ion. It was assumed that I^- was oxidized to I_2 ($E^{\circ}_{1/2} = 0.26$ V[9] vs. SCE) {or I_3^- ($E^{\circ}_{1/2} = 0.06$ V[9])} and TCNE ($E^{\circ}_{1/2} = 0.26$ V) was reduced.[3,10] In contrast to amorphous $[V(TCNE)_x]$, $[Mn(TCNE)_2]$, and $[Fe(TCNE)_2]$ magnets synthesized by the iodide route exhibit isomorphous powder X-ray diffraction patterns suggesting some crystallinity, and the structure of $[Fe(TCNE)_2]$ was recently solved and shown to be $[Fe(TCNE)\{C_4(CN)_8\}_{1/2}]$.[11]

Due to the greater potential needed to oxidize Cl^- ($E^{\circ}_{1/2} = 0.34$ V[12]) with respect to I^- in MeCN, reduction of TCNE with MCl_2 (M = Fe, Mn, Co, Ni) should not occur. Nonetheless, as reported herein, TCNE reacts with $[FeCl_2(NCMe)_2]$ (**1**) in MeCN to reduce TCNE to form a layered network

---

[a] Dr. K. I. Pokhodnya, M. Bonner, Prof. J. S. Miller
Department of Chemistry, University of Utah
Salt Lake City, UT 84112-0850 (USA)
Fax: (+1) 801-581-8433
E-mail: jsmiller@chem.utah.edu

[b] Dr. A. G. DiPasquale, Prof. A. L. Rheingold
Department of Chemistry and Biochemistry
University of California, San Diego, La Jolla, CA 92093-0358 (USA)

structure similar to previously reported $[\mathrm{Fe^{II}\{C_4(CN)_8\}(NCMe)_2}]\cdot z\,\mathrm{MeCN}$,[13] and reacts in $\mathrm{CH_2Cl_2}$ to form magnetically ordered $[\mathrm{Fe^{II}(TCNE^{\bullet-})(NCMe)_2}][\mathrm{Fe^{III}Cl_4}]$ ($T_c = 90$ K).[14]

To understand the reaction in MeCN requires a detailed understanding of the redox properties of the $\mathrm{MCl_2}$ (M = Mn, Fe, Co) acetonitrile solvates, and herein the electrochemical and spectroscopic characterization of $\mathrm{MCl_2}$ as their acetonitrile solvates, and reaction of TCNE and compound **1** to form $[\mathrm{Fe^{II}\{C_4(CN)_8\}(NCMe)_2}]$ and its magnetic properties are reported.

Results and Discussion

As noted in the introduction, the reaction of TCNE with $[\mathrm{FeCl_2(NCMe)_2}]$ (**1**) in a $\mathrm{CH_2Cl_2}$ slurry forms magnetically ordered $[\mathrm{Fe(TCNE)(NCMe)_2}][\mathrm{FeCl_4}]$ ($T_c = 90$ K).[14] Albeit exciting due to the discovery of a new family of organic-based magnets, it was unexpected, and due to the greater coordinating ability of MeCN and poor solubility of **1** in $\mathrm{CH_2Cl_2}$, we sought to study this chemistry in MeCN. In particular, identification of the reducing agent was sought. Chain-structured $[\mathrm{MCl_2(NCMe)_2}]$ (M = Mn, Fe) was isolated by slow diffusion of $\mathrm{Et_2O}$ into a concentrated solution of $\mathrm{MCl_2}$ in acetonitrile.[15] In contrast, the $\mathrm{Co^{II}Cl_2}$ solvate crystallizes as $[\mathrm{Co^{II}(NCMe)_6}][\mathrm{Co^{II}Cl_3(NCMe)}]_2$,[16] in accord with an earlier electronic absorption spectroscopic study suggesting that a dilute solution $\mathrm{CoCl_2}$ in MeCN exists as an equilibrium of neutral $[\mathrm{Co^{II}Cl_2(NCMe)_2}]$ and ionic $[\mathrm{Co^{II}Cl_3(NCMe)}]^-$ and $[\mathrm{Co^{II}(NCMe)_6}]^{2+}$ species.[17] The solution chemistry and electrochemistry of $\mathrm{MCl_2}$ (M = Mn, Fe, Co) as well as the reaction of their solvates with TCNE is studied. The reaction of compound **1** with TCNE leads to the formation of $[\mathrm{Fe^{II}\{C_4(CN)_8\}(NCMe)_2}]\cdot\mathrm{MeCN}$ (**4**) and not $[\mathrm{Fe(TCNE)(NCMe)_2}][\mathrm{FeCl_4}]$. Furthermore, there was no reaction with the Co– and Mn–MeCN solvates. The genesis of this was elucidated from a study of the electronic and electrochemical properties of MeCN solvates of $\mathrm{MCl_2}$ (M = Mn, Fe, Co).

Compound **4** exhibits two ν_{CN} absorptions at 2308 and 2281 $\mathrm{cm^{-1}}$, characteristic to coordinated MeCN, and two more intense peaks at 2213 and 2153 $\mathrm{cm^{-1}}$, characteristic to coordinated $[\mathrm{TCNE}]^{\bullet-}$, as previously reported for a different polymorph of compound **4**.[13,15,18] The peaks at 1408 and 1367 $\mathrm{cm^{-1}}$ most probably can be assigned as deformation δ-$\mathrm{CH_3}$ modes in MeCN, while peaks at 1029, 930, and 795 $\mathrm{cm^{-1}}$ also most probably are less characteristic modes of this ligand.[19] In contrast, peaks at 1310, 1202, and 558 $\mathrm{cm^{-1}}$ are attributed to the $[\mathrm{C_4(CN)_8}]^{2-}$ ion.

The single-crystal structural analysis of **4** reveals the composition as $[\mathrm{Fe\{C_4(CN)_8\}(NCMe)_2}]\cdot\mathrm{MeCN}$ in accord with the IR spectra. A polymorph of it has been reported,[13] but the symmetry and the unit-cell parameters of **4** are different. Nonetheless, the structural motif for both polymorphs is similar. Both polymorphs are composed of two-dimensional coordination polymeric layers of hexacoordinate $\mathrm{Fe^{II}}$ ions equatorially bonded to the four terminal μ_4-$[\mathrm{C_4(CN)_8}]^{2-}$ nitrile groups derived from the σ-dimerization of two $[\mathrm{TCNE}]^{\bullet-}$ radicals ions. This forms 15-membered rings. The two apical octahedral positions are occupied by MeCN molecules. In contrast to the earlier reported structure, as well as its Mn analogue,[13] in which all μ_4-$[\mathrm{C_4(CN)_8}]^{2-}$ dianions were equivalent, there are two nonequivalent μ_4-$[\mathrm{C_4(CN)_8}]^{2-}$ units (I and II, Figure 1 top) for **4**, and I is disordered about the midpoint of the C5−C5′ bond. As a result, this new polymorph has a less symmetrical monoclinic unit cell and almost doubled unit-cell volume. Key bond length and bond angle information is provided in Table 1.

The two independent μ_4-$[\mathrm{C_4(CN)_8}]^{2-}$ ions present in **4** contain long central C−C bonds, 1.656(12) and 1.598(10) Å for I and II, respectively, that join two TCNE units; both carbon atoms involved are $\mathrm{sp^3}$ hybridized. The average Fe−N dis-

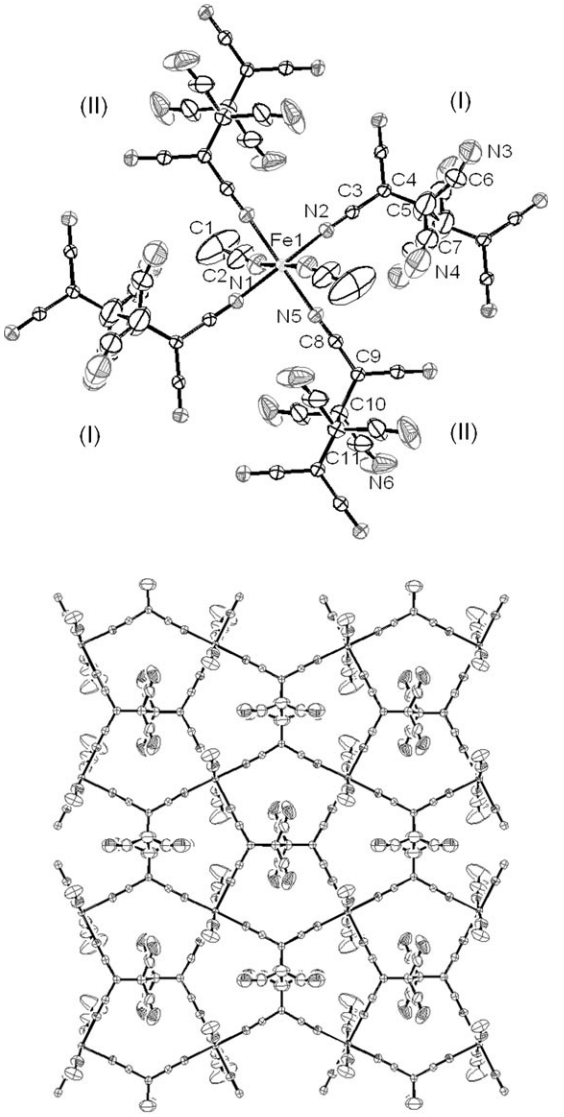

Figure 1. Top: Atom labeling ORTEP plot of the asymmetric unit in compound **4** with atoms depicted as 50 % probability ellipsoids. Bottom: crystal packing diagram within one two-dimensional layer (see text).

Table 1. Selected bond lengths [Å] and angles [°] for **4**.

Fe1–N1	2.186(4)	C3–C4	1.382(4)	N2-Fe1-N2	180.0
Fe1–N2	2.082(3)	C4–C5	1.610(7)	N2-Fe1-N5	89.93(10)
Fe1–N5	2.148(3)	C5–C7	1.508(8)	N2-Fe1-N5	90.08(10)
N1–C2	1.106(6)	C5–C6	1.513(9)	N2-Fe1-N5	90.07(10)
N2–C3	1.131(4)	C5–C5′	1.656(12)	C6-C5-C4	120.4(4)
N3–C6	1.085(8)	C8–C9	1.393(4)	C7-C5-C4	120.5(4)
N4–C7	1.124(8)	C9–C10	1.523(6)	C5-C5′-C4	102.4(5)
N5–C8	1.147(4)	C10–C11	1.474(5)	C11-C10-C9	111.6(3)
N6–C11	1.132(6)	C10–C10′	1.598(10)	C9-C10′-C10	114.2(5)

tance to the μ$_4$-[C$_4$(CN)$_8$]$^{2-}$ ligand is 2.115 Å, while the 2.186(4) Å Fe–N distance to the MeCN ligand is 0.071 Å longer. The other polymorph, albeit disordered, has a long central C–C bond of 1.627(14) Å, and Fe–N distances to MeCN of 2.273(6) Å, and to μ$_4$-[C$_4$(CN)$_8$]$^{2-}$ of 2.218(7) Å. While the C–C bond is comparable in both structures, the Fe–N distances to both ligands are ≈0.1 Å shorter in the new polymorph. It should be noted that structurally similar [Mn{C$_4$(CN)$_8$}(NCMe)$_2$]·CH$_2$Cl$_2$ has an average long central C–C bond of 1.569 Å, and Mn–N distances to MeCN of 2.235 Å, and to μ$_4$-[C$_4$(CN)$_8$]$^{2-}$ of 2.218 Å.[13]

Adjacent two-dimensional planes are eclipsed (Figure 1, bottom), and the interlayer Fe···Fe separation is 8.059 Å, while the shortest intralayer Fe···Fe distance is 8.126 Å. It should be noted that all Fe ions within the plane are interconnected through a five-atom NC-C-CN fragment of the [C$_4$(CN)$_8$]$^{2-}$ ligands, suggesting a superexchange coupling pathway. In contrast, large interlayer separation implies only weak dipole–dipole interlayer coupling; therefore, a strong anisotropy of magnetic properties is anticipated.

The 2–300 K temperature-dependent magnetic susceptibility, $\chi(T)$ of **4** at 1 kOe applied field is reported as $\chi T(T)$, Figure 2. The 300 K value of χT is 3.91 emuK mol^{-1}, which is close to that expected for high-spin octahedral Fe^{II} with weak spin-orbit coupling (3.85 emuK mol^{-1}).[20] The $\chi^{-1}(T)$ values can be fit to the Curie–Weiss expression, $\chi \propto (T-\theta)^{-1}$, with a negative θ of −13.3 K implying substantial antiferromagnetic coupling.

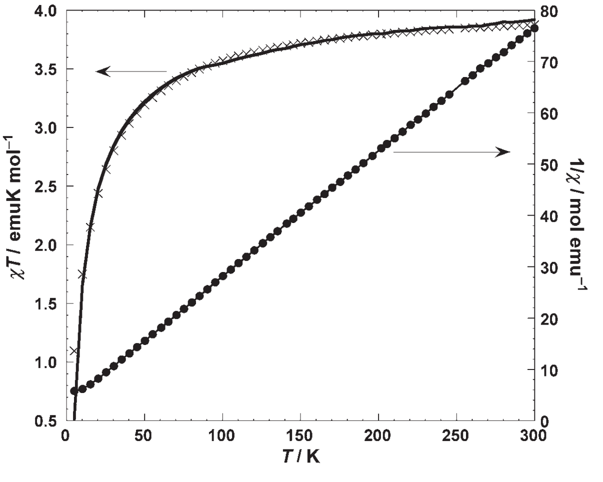

Figure 2. Observed $\chi T(T)$ (×) and $\chi^{-1}(T)$ (●) for compound **4** in 1 kOe applied field. Solid lines are fits to Curie–Weiss law with $g=2.235$, $\theta=-13.3$ K, and TIP$=1.5\times10^4$ emu mol^{-1} (TIP = temperature independent paramagnetism).

The low-temperature behavior of $\chi(T)$ at low field is more complex (Figure 3) and deviates from Curie–Weiss behavior. The zero-field cooled magnetization, $M_{ZFC}(T)$, at 5 Oe rises slowly upon cooling and below 8.5 K increases abruptly with a sharp maximum at 7.8 K, and then on further cooling almost vanishes below 6 K, suggesting an antiferromagnetic ground state. The magnetic transition reveals itself as a more resolved sharp peak at the same temperatures in the in-phase $\chi'(T)$ component of the ac susceptibility (10 to 1000 Hz frequency range). The peak position is frequency independent implying good sample crystallinity. The out-of-phase component of the ac susceptibility ($\chi''(T)$) is very small (close to the magnetic property measurement system (MPMS) sensitivity limit) in the vicinity of transition, and vanishes at lower temperatures, which is also in accord with an antiferromagnetic ground state. As expected, the field dependence of magnetization, $M(H)$, at 2 K (Figure 4) is linear with the field, but above ≈25 kOe it starts to deviate from linearity indicating the onset of the field-induced transition, most probably, metamagnetic-like in origin.

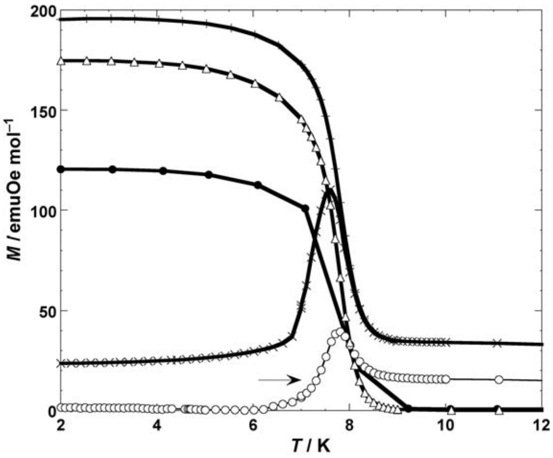

Figure 3. Temperature dependences of zero-field-cooled (χ_{ZFC}) [5 (○, 250 Oe (×)], field-cooled (χ_{FC}) [5 (●), 250 Oe (+)], and remanent (χ_r)(△) magnetizations for compound **4** at different applied fields. χ_{ZFC} at 5 Oe (○) was multiplied by 20.

Interestingly, cooling to 2 K in a small (5 Oe) field (field-cooled magnetization; $M_{FC}(T)$) reveals that $M_{FC}(T)$ is very different from $M_{ZFC}(T)$ for **4**. Its value at 2 K is 121 emu Oe mol^{-1} and it decreases slightly upon warming before sharply dropping above 6 K; above 9 K the $M_{FC}(T)$ and $M_{ZFC}(T)$ values coincide. The remanent magnetization ($M_r(T)$) measured in a zero external field on warming after the sample was cooled to 2 K in a 250 Oe field exhibits a similar behavior. The presence of a substantial remanence at low temperatures is in accord with an observed magnetic hysteresis ($H_{cr}=2$ kOe) at 2 K. It should be noted that $M_{ZFC}(T)$ at 2 K increases much faster with increasing field

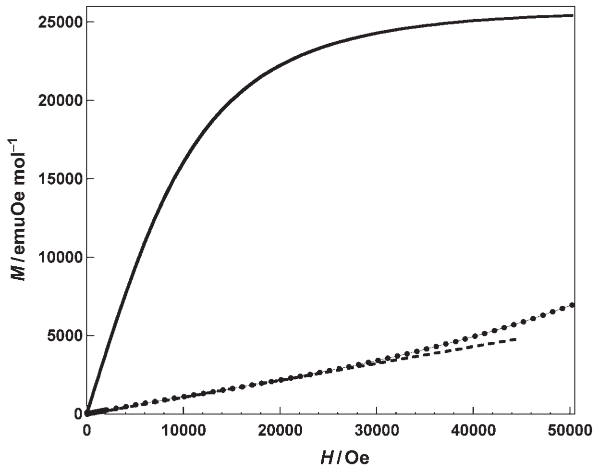

Figure 4. Magnetization field dependence $M(H)$ (●) of compound **4** at 2 K and that calculated from the Brillouin function for $S=2$ and $g=2.3$ (——). Dotted line is a visual guide.

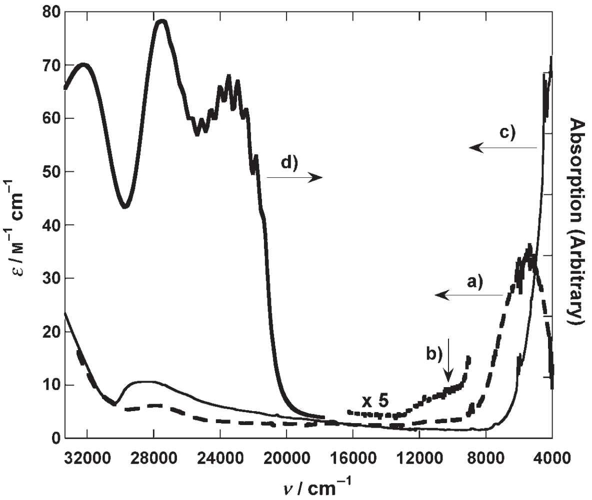

Figure 5. a) Absorption spectrum of **1**; b) scaled spectrum of **1** in the region 9000 to 16000 cm^{-1} (····); c) absorption spectrum of $[NEt_4]_2[Fe^{II}Cl_4]$ in MeCN; and d) absorption spectrum of the TCNE + $[NEt_4]_2[Fe^{II}Cl_4]$ reaction products in MeCN (——), see text.

than $M_{ZC}(T)$ suggesting that both should collapse in the vicinity of critical field for the field-induced magnetic transition.

Thus, we assume that within the μ_4-$[C_4(CN)_8]^{2-}$ layer, the Fe^{II} ions are ferromagnetically coupled through five-atom NC-C-CN superexchange pathways, and the magnetization is perpendicular to the layer. In contrast, the interaction between spins in the adjacent layers is relatively weak and antiferromagnetic in origin resulting in the antiferromagnetic ground state similar to that observed in $FeCl_2$ and other classical metamagnets.[21] However, application of the magnetic field results in an irreversible transition of **4** to a metastable state, most probably a slightly canted antiferromagnet in which magnetization vectors of the adjacent layers (directed perpendicular to the layer) are slightly non-colinear, and the fraction of this state increases with the field at the expense of the antiferromagnetic phase. Since the two pairs of molecules in the **4** unit cell are related by the inversion center, canting should not occur. Therefore, it is assumed to be related to structural anisotropy and defects, MeCN ligand losses, and so forth. The detailed study of this effect is in progress.

Electronic spectra of $FeCl_2$ solvates: To gain insight into the mechanism of TCNE reduction by $FeCl_2$, the nature of iron(II) chloride species existing in equilibrium in MeCN needs to be identified. The electronic spectrum of $[FeCl_2(NCMe)_2]$ (**1**) dissolved in MeCN was studied between 4000 and 33000 cm^{-1}, and compared with that for $[NEt_4]_2[Fe^{II}Cl_4]$ (Figure 5). The spectrum of **1** exhibits a broad absorption at ≈5400 cm^{-1} in accord with its tetrahedral geometry. The shift to higher frequency of this d–d transition from that at ≈4050 cm^{-1} for the tetrahedral $[Fe^{II}Cl_4]^{2-}$[22] ion is consistent with $[Fe^{II}Cl_3(NCMe)]^-$ being present in MeCN, as MeCN is a strong-field ligand with respect to Cl^-.[23] In the series of tetrahedral complexes of $[Fe^{II}Cl_4]^{2-}$, $[Fe^{II}(L^+CH_3)Cl_3]$, and $[Fe^{II}Q_2Cl_2]$ (L = 1,4-diazabicyclo[2.2.2]octane; Q = quinuclidine), a similar regular blue shift (4050→4900→7150 cm^{-1}) of the d–d transition was observed due to successive substitution of Cl by a nitrogen-donor ligand.[24] Therefore, the ≈5400 cm^{-1} absorption was assigned to the d–d transition for tetrahedral $[Fe^{II}Cl_3(NCMe)]^-$. The low absorption value at 4050 cm^{-1} implies a vanishing concentration of the $[Fe^{II}Cl_4]^{2-}$ ion in the solution of **1** in MeCN in accord with CV data (see below). Unfortunately, a strong MeCN overtone absorption in the near-IR region (deep narrow peaks) is observed, and it is difficult to compensate for this even using a 1 mm path length (the thickness decrease is limited by the solubility of **1**) making attempts to find absorptions that can be assigned to the $[Fe^{II}Cl_x(NCMe)_{4-x}]^{2-x}$ ($x=1$, 2) tetrahedral species challenging. Interestingly, a weak shoulder characteristic of the $^5T_{2g}\rightarrow{}^5E_g$ transition in $[Fe^{II}(MeCN)_6]^{2+}$ is clearly visible at ≈11000 cm^{-1}[25] suggesting that this specie is also present.

Due to the low solubility of $[MnCl_2(NCMe)_2]$ (**2**) in MeCN and the strong MeCN overtone absorption, the near-IR solution spectrum was difficult to interpret, while in Nujol the tetrahedral d–d transition was not seen because of the octahedral Mn^{II} environment.[15] In contrast, the near-IR spectrum of **3** exhibits absorptions at 5000 and 7400 cm^{-1} assigned to a d–d transitions in the $[CoCl_3(MeCN)]^-$ ion in accord with those (4900 and 7800 cm^{-1}) observed for $[Co^{II}(L^+H)Cl_3]$.[24]

Electrochemical properties: To elucidate the redox properties of the $M^{II}Cl_2$–MeCN (M = Fe, Mn, Co) adducts, the cyclic voltammograms (CV) of solutions of these adducts in acetonitrile were measured; the results are summarized in Table 2. The CV of **1** consists of at least three partially resolved quasi-reversible waves at 0.86, 0.48, and 0.21 V versus SCE, Figure 6. The last wave potential is 0.17 V higher than that for the Fe^{III}/Fe^{II} couple for both $[Fe^{III}Cl_4]^-$

Table 2. Electrochemical data for $[NEt_4]_2[Fe^{II}Cl_4]$, $[NEt_4][Fe^{III}Cl_4]$, **1**, **2**, and **3** [vs. SCE] in MeCN.[a]

Compound	E_{pa} [V]	E_{pc} [V]	ΔE_p [V]	$E_{1/2}$ [V]
$[NEt_4]_2[Fe^{II}Cl_4]$	−0.03	0.12	0.15	0.04
$[NEt_4][Fe^{III}Cl_4]$	-0.04	0.10	0.14	0.03
$[Fe^{II}Cl_2(NCMe)_2]$ (**1**) $[Fe^{II}Cl_3(NCMe)]^-$	0.13	0.28	0.15[b]	0.21
$[Fe^{II}Cl_2(NCMe)_2]$ (**1**) $[Fe^{II}Cl_2(NCMe)_2]$	0.40	0.55	0.15[b]	0.48
$[Fe^{II}Cl_2(NCMe)_2]$ (**1**) $[Fe^{II}Cl(NCMe)_3]^+$	0.78	0.93	0.15[b]	0.86
$[Mn^{II}Cl_2(NCMe)_2]$ (**2**)	1.83	0.67	0.58	1.25
	−0.96	0.16	1.00	−0.46
$[Co^{II}(NCMe)_6][Co^{II}Cl_3(NCMe)]_2\cdot MeCN$	−0.71	0.25	0.96	−0.23
TCNE	0.23	0.31	0.08	0.26

[a] With 0.1 M $[NBu_4][BF_4]$. [b] Since the wave was only partially resolved, ΔE_p was assumed to be 0.15 V similar to that for $[FeCl_4]^{2-}$.

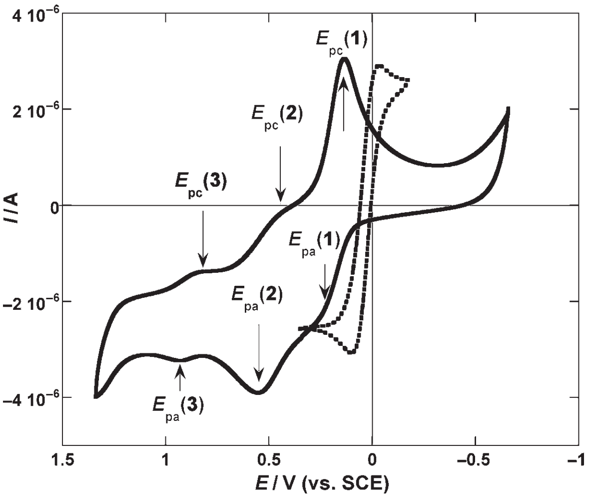

Figure 6. CV (solid line) of **1** in MeCN containing 0.1 M $[NBu_4][BF_4]$; sweep rate 50 mV s^{-1}. CV of $[NEt_4]_2[Fe^{II}Cl_4]$ (dotted line) is shown for comparison.

and $[Fe^{II}Cl_4]^{2-}$ ions;[26] therefore, the presence of $[Fe^{II}Cl_4]^{2-}$ can be ruled out. MeCN stabilizes lower oxidation states due to a back donation {for example, the redox potential of the Fe^{III}/Fe^{II} couple is +1.86 V (vs. SCE) for $[Fe^{II}(NCMe)_6]^{2+}$}.[27] Therefore, as discussed above, **1** in MeCN exists as an equilibrium of differently charged (as well as neutral) tetrahedral $[Fe^{II}Cl_x(NCMe)_{4-x}]^{2-x}$ $(1 \leq x \leq 3)$ species and the reduction potential for these species increases with decreasing x. Thus, the three observed CV waves are assigned as Fe^{III}/Fe^{II} one-electron reduction potentials for $[Fe^{II}Cl_x(NCMe)_{4-x}]^{2-x}$ $(1 \leq x \leq 3)$, respectively. The lack of a reduction wave at 0.04 V implies a negligible (if any) concentration of $[FeCl_4]^{2-}$ when **1** is dissolved in MeCN, although, $[Fe^{II}(NCMe)_6]^{2+}$ is present, as observed in the electronic absorption spectrum (Figure 5). The gradual increase of the reduction potential of $[Fe^{II}Cl_x(NCMe)_{4-x}]^{2-x}$ species with decreasing x is consistent with step-like substitution of Cl with MeCN.

The CV of **2** displays an irreversible oxidation wave at ≈1.25 V and a quasi-reversible reduction wave at ≈−0.46 V. The first wave was assigned to the oxidation of the Mn^{II} to Mn^{III}, since the same process in $[Mn^{II}Cl_4]^{2-}$ ion has a slightly lower potential of 1.1 V.[28a] The second wave, most probably, is a one-electron Mn^{II} to Mn^{I} reduction. The two-electron reduction process of Co^{II} to Co^{0} is observed in the CV of (**3**) at −0.23 V, which is in accord with a handbook value.[28c] The Co^{III}/Co^{II} redox couple potential is beyond the studied range. Thus, comparing the half-wave potentials of the studied MCl_2–acetonitrile (M = Mn, Fe, Co) adducts with that for TCNE/$[TCNE]^{\cdot-}$ (0.26 V, Table 2) only $[Fe^{II}Cl_3(NCMe)]^-$ (and $[Fe^{II}Cl_4]^{2-}$, if present) could reduce TCNE to $[TCNE]^{\cdot-}$.

Reaction with TCNE: When TCNE was added to a colorless solution of $[NEt_4]_2[Fe^{II}Cl_4]$ in MeCN, the solution immediately turned orange, suggesting the presence of $[TCNE]^{\cdot-}$. This was confirmed from the electronic spectrum, which has a broad electronic transition at ≈23 400 cm^{-1} with a number of sharp vibronic features characteristic of $[TCNE]^{\cdot-}$ (Figure 5).[29] In addition, two strong lines at 32 250 and 27 600 cm^{-1} that are characteristic of $[Fe^{III}Cl_4]^-$ ion[30] are observed. Since both $[TCNE]^{\cdot-}$ and $[Fe^{III}Cl_4]^-$ transitions have similar molar extinction, the close absorption values of these peaks suggests a comparable concentration of these species in the studied solution, implying a quantitative TCNE→$[TCNE]^{\cdot-}$ transformation in accord with half-wave potential values. It should be noted that both compounds remain in solution for at least a week, and no precipitate was formed. Hence, the reaction given in Equation (1) occurs with a 0.23 V favorable redox potential.

$$[Fe^{II}Cl_4]^{2-} + TCNE \rightarrow [Fe^{III}Cl_4]^- + [TCNE]^{\cdot-} \quad (1)$$

In contrast, when TCNE was added to a colorless solution of **1** in MeCN it immediately turned yellow, and then became dark orange within few minutes; eventually a pale green precipitate formed. The CN bond stretching modes (2308, 2281, 2213, and 2153 cm^{-1}) in the IR spectrum of the precipitate and its powder XRD pattern are consistent with the formation of compound **4** reported above.

The solution chemistry of $[Fe^{II}Cl_2(NCMe)_2]$ (**1**) was investigated to identify why $[Fe^{II}\{C_4(CN)_8\}(NCMe)_2]$ (**4**) forms, but only the one-electron transfer redox reaction occurs when $[Fe^{II}Cl_4]^{2-}$ is used to reduce TCNE. Compound **1** dissolves in MeCN and exhibits a weak shoulder characteristic for the $^5T_{2g} \rightarrow {}^5E_g$ transition in $[Fe^{II}(MeCN)_6]^{2+}$ at ≈11 000 cm^{-1} in its UV/Vis spectrum (Figure 5).[31] Comparing its molar extinction coefficient ($\varepsilon = 9.4\,M^{-1}\,cm^{-1}$) with the observed value (≈1 M^{-1} cm^{-1}), only ≈11 % of Fe^{II} exists in solution in this octahedral form. Thus, in MeCN, compound **1** forms $[Fe^{II}(NCMe)_6]^{2+}$ and $[Fe^{II}Cl_3(NCMe)]^-$ [Eq. (2)]. The reduction potential of $[Fe^{II}Cl_3(NCMe)]^-$ (0.21 V) is sufficient to reduce TCNE [Eq. (3)] and $[Fe^{II}(NCMe)_6]^{2+}$

reacts with $[TCNE]^{\bullet-}$ precipitating network-structured compound **4** [Eq. (4)]. Finally, the formed $Fe^{III}Cl_3$ [Eq. (3)] in a polar aprotic solvent like MeCN forms $[Fe^{III}Cl_4]^-$ and $[Fe^{III}Cl_2(NCMe)_n]^+$, [Eq. (5)].[32] Therefore, the presence of $[Fe^{II}(NCMe)_6]^{2+}$ in a solution of **1** in MeCN is crucial for the formation of the $[Fe\{C_4(CN)_8\}]$ network structure, as it does not form when $[Fe^{II}(NCMe)_6]^{2+}$ is not present, [Eq. (1)]. To verify this hypothesis, $[Fe^{II}(NCMe)_6]^{2+}$ was added to $[TCNE]^{\bullet-}$ in MeCN and it led to an immediate precipitate of compound **4**, consistent with this reaction sequence.

$$3\,[Fe^{II}Cl_2(NCMe)_2] + 2\,MeCN \rightarrow 2\,[Fe^{II}Cl_3(NCMe)]^- + [Fe^{II}(NCMe)_6]^{2+} \quad (2)$$

$$2\,[Fe^{II}Cl_3(NCMe)]^- + 2\,TCNE \rightarrow 2\,Fe^{III}Cl_3 + 2\,[TCNE]^{\bullet-} \quad (3)$$

$$[Fe^{II}(NCMe)_6]^{2+} + 2\,[TCNE]^- \rightarrow [Fe^{II}\{C_4(CN)_8\}(NCMe)_2]\,(s) + 4\,MeCN \quad (4)$$

$$2\,Fe^{III}Cl_3 + n\,MeCN \rightarrow [Fe^{III}Cl_4]^- + [Fe^{III}Cl_2(NCMe)_n]^+ \quad (5)$$

Experimental Section

All manipulations were performed under an inert nitrogen atmosphere (<1 ppm O_2 and <1 ppm H_2O) using standard Vacuum Atmospheres DriLab glove boxes. All solvents were sparged with nitrogen and passed over two columns of activated alumina prior to use to remove traces of oxygen and water.[33] $[FeCl_2(NCMe)_2]$ (**1**), $[MnCl_2(NCMe)_2]$ (**2**) and $[Co(NCMe)_6][CoCl_3(NCMe)]_2$ (**3**) were synthesized as previously described.[15] The CryoLoop and Paratone-N oil were obtained from Hampton Research.

$[Fe^{II}\{C_4(CN)_8\}(NCMe)_2]\cdot MeCN$ (4): A solution of compound **1** (99.8 mg; 0.48 mmol) in MeCN (≈5 mL) was added dropwise to a stirred solution of TCNE (40.8 mg; 0.32 mmol) in MeCN (≈3 mL). The reaction immediately turned orange and a light-colored precipitate slowly formed. The mixture was stirred for 12 h and vacuum filtered to isolate the solid. The light green solid (yield ≈64%) was washed with minimal amount of MeCN and stored in a vial slightly wet to keep the product solvated. The compound looses solvent rapidly at ambient conditions; this results in broadening of powder XRD as well as IR absorption peaks suggesting poor crystallinity. IR (KBr): $\tilde{\nu}=2308$ m, 2281 (m), 2213 (s), 2153 (s), 1408 (m), 1368 (m), 1310 (m), 1201 (m), 930 (m), 795 (m), 558 cm^{-1} (m). Single crystals of **4** were grown by slow diffusion or by means of placing the reagents in an H-tube with a $MeCN/CH_2Cl_2$ mixture as a solvent. Dark green plates of 0.5×0.5×0.1 mm in size were collected after ≈30 days.

X-ray analysis of compound 4: A 0.5×0.3×0.1 mm dark green plate was mounted on a CryoLoop with Paratone oil. Data collection was done at room temperature due to irreversible phase changes at low temperatures. The crystal-to-detector distance was 60 mm and exposure time was 10 s per frame with a scan width of 0.3°. The data were integrated with the Bruker SAINT software program and corrected for absorption by the Bruker SADABS software program. Solution by direct methods (SIR-2004)[34] produced a complete heavy-atom phasing model consistent with the proposed structure. All non-hydrogen atoms were refined anisotropically by full-matrix least-squares methods (SHELXL-97).[35] All hydrogen atoms were placed using a riding model and their positions constrained relative to their parent atom by using the appropriate HFIX command in SHELXL-97.[35] A summary of data collection parameters for **4** is given in Table 3. In addition to the two molecules of MeCN coordinated to Fe, the asymmetric unit contains one molecule of MeCN per Fe atom. The solvent was highly disordered and could only be properly rendered using SQUEEZE, which treats the solvent as a diffuse contribution, but does not provide individual atom sites. However, the solvent's contributions are included in the computations of intensive properties.

Table 3. Crystallographic data for $[Fe^{II}\{C_4(CN)_8\}(NCMe)_2]\cdot MeCN$ (**4**).

crystal system	monoclinic	Z	4
formula	$FeC_{18}N_{11}H_9$	T [K]	295(2)
space group	$C2m$	V [Å^3]	2138.6(5)
a [Å]	16.253(2)	ρ_{calcd} [g cm^{-3}]	1.356
b [Å]	16.3331(2)	$R1^{[a]}$	0.0609
c [Å]	8.0598(11)	$wR2^{[b]}$	0.1869
β [°]	91.514(2)	$S^{[c]}$	1.104

[a] $R1=\Sigma||F_o|-|F_c||/\Sigma|F_o|$. [b] $wR2=[\Sigma(w(F_o^2-F_c^2)^2)/\Sigma(F_o^2)^2]^{1/2}$. [c] $S=[\Sigma(w(F_o^2-F_c^2)^2/(n-p)]^{1/2}$.

CCDC-632333 (**4**) contains the supplementary crystallographic data for this paper. These data can be obtained free of charge from The Cambridge Crystallographic Data Centre via www.ccdc.cam.ac.uk/data request/cif.

Physical properties: Electronic absorption spectra were recorded on HP-8452a spectrometer in the UV/Vis range and on a Cary 17 spectrophotometer equipped with OLIS data acquisition system in the near-IR range. In the latter case 1 mm path length quartz cuvettes were used to avoid excessive solvent absorption. Far and mid infrared spectra (50 to 4000 ± 1 cm^{-1}) were obtained on a Bruker Tensor 37 FT spectrophotometer as either KBr pellets or Nujol mulls.

Electrochemical cyclic voltammetry were performed on an Epsilon EC V120 potentiostat/galvanostat with $[NBu_4][BF_4]$ (0.1 M) as supporting electrolyte, and Pt and Pt-wire as working and counter electrodes, respectively. All potentials were measured versus the Ag^+/Ag reference electrode, with 0.01 M $AgNO_3$ in MeCN, which was separated from both working and counter electrodes by a Vycor tip. The ferrocenium/ferrocene couple was used as the internal standard, and all potential are reported with respect to SCE. Scan rates vary from 25 to 100 $mV\,s^{-1}$ in the range of −1.5 to +1.0 V.

The 2–300 K magnetic susceptibility was determined on a Quantum Design MPMS-5XL 5 T SQUID as previously described.[36] In addition to correcting for the diamagnetic contribution from the sample holder, and core diamagnetic correction of -187×10^{-6} emu mol^{-1} for compound **4** was used.

Acknowledgements

The authors are grateful for helpful discussions with Fernando Palacio (Zaragoza), and the continued partial support by the Department of Energy Division of Materials Science (Grant Nos. DE-FG03-93ER45504 and DE-FG02-01ER4593), and the U.S. Air Force Office of Scientific Research (Grant No. F49620-03-1-0175).

---

[1] R. M. White, *J. Appl. Phys.* **1985**, *57*, 2996; W. E. Wallace, *J. Less-Common Met.* **1984**, *100*, 85; M. Brown, *High-Tech Mater Alert* **2000**, *17*, 10.

[2] For example, V. I. Ovcharenko, R. Z. Sagdeev, *Russ. Chem. Rev.* **1999**, *68*, 345; M. Kinoshita, *Philos. Trans. R. Soc. London Ser. A* **1999**, *357*, 2855; J. S. Miller, A. J. Epstein, *Chem. Commun.* **1998**,

1319; J. S. Miller, A. J. Epstein, *Chem. Eng. News* **1995**, *73*(40), 30; S. J. Blundell, F. L. Pratt, *J. Phys. Condens. Matter* **2004**, *16*, R771; J. A. Crayston, J. N. Devine, J. C. Walton, *Tetrahedron* **2000**, *56*, 7829. J. S. Miller, A. J. Epstein, *Angew. Chem.* **1994**, *106*, 339; *Angew. Chem. Int. Ed. Engl.* **1994**, *33*, 385.

[3] J. Zhang, J. Ensling, V. Ksenofontov, P. Gütlich, A. J. Epstein, J. S. Miller, *Angew. Chem.* **1998**, *110*, 676; *Angew. Chem. Int. Ed.* **1998**, *37*, 657; J. S. Miller, unpublished results.

[4] a) J. M. Manriquez, G. T. Yee, R. S. McLean, A. J. Epstein, J. S. Miller, *Science* **1991**, *252*, 1415; b) J. S. Miller, G. T. Yee, J. M. Manriquez, A. J. Epstein in the *Proceedings of Nobel Symposium #NS-81: Conjugated Polymers and Related Materials: The Interconnection of Chemical and Electronic Structure*, Oxford University Press, **1993**, p. 461; J. S. Miller, G. T. Yee, J. M. Manriquez, A. J. Epstein, *La Chim. La Ind.* **1992**, *74*, 845; c) J. Zhang, P. Zhou, W. B. Brinckerhoff, A. J. Epstein, C. Vazquez, R. S. McLean, J. S. Miller, *ACS Symp. Ser.* **1996**, *644*, 311.

[5] Hysteretic magnetic behavior was reported for reaction products of TCNE with Cr, Nb, and Mo at low temperatures (in case of Cr it was also observed at 300 K) [D. de Caro, C. Faulmann, L. Valade, *Chem. Eur. J.* **2007**, *13*, 1650]; however, the composition and critical temperatures of these compounds were not identified; reporting the hysteresis loop without the determination of magnetization saturation values does not provide better understanding of the magnetic behavior, since it could be related to magnetic impurities.

[6] S. A. Wolf, *J. Supercond.* **2000**, *13*, 195; G. Prinz, *Science* **1998**, *282*, 1660. H. Ohno, F. Matsukura, *Solid State Commun.* **2001**, *117*, 179.

[7] V. N. Prigodin, N. P. Raju, K. I. Pokhodnya, J. S. Miller, A. J. Epstein, *Adv. Mater.* **2002**, *14*, 1230; N. P. Raju, T. Savrin, V. N. Prigodin, K. I. Pokhodnya, J. S. Miller, A. J. Epstein, *J Appl. Phys.* **2003**, *93*, 6799; C. Tengstedt, M. P. de Jong, A. Kanciurzewska, E. Carlegrim, M. Fahlman, *Phys. Rev. Lett.* **2006**, *96*, 057209.

[8] S. Pohl, W. Saak, *Z. Naturforsch. B* **1984**, *39*, 1236. F. Weller, H.-J. Mai, K. Dehniche, *Z. Naturforsch. B* **1996**, *51*, 298.

[9] P. G. Desideri, L. Lepri, D. Heimler in *Encyclopedia of Electrochemistry of the Elements* (Ed.: A. J. Bard), Marcel Dekker, New York, **1973**, p. 95.

[10] O. W. Webster, W. Mahler, R. E. Benson, *J. Org. Chem.* **1960**, *25* 1470.

[11] J.-H. Her, P. W. Stephens, K. I. Pokhodnya, M. Bonner, J. S. Miller, *Angew. Chem.* **2007**, *119*, 1543; *Angew. Chem. Int. Ed.* **2007**, *46*, 1521.

[12] T. Mussini, G. Faita in *Encyclopedia of Electrochemistry of the Elements* (Ed.: A. J. Bard), Marcel Dekker, New York, **1973**, p. 12.

[13] J. Zhang, L. M. Liable-Sand, A. L. Rheingold, R. E. Del Sesto, D. C. Gordon, B. M. Burkhard, J. S. Miller, *Chem. Commun.* **1998**, 1385.

[14] K. I. Pokhodnya, M. Bonner, J.-H. Her, P. W. Stephens, J. S. Miller, *J. Am. Chem. Soc.* **2006**, *128*, 15592.

[15] K. I. Pokhodnya, M. Bonner, A. G. DiPasquale, A. L. Rheingold, J.-H. Her, P. W. Stephens, J.-W. Park, B. S. Kennon, A. M. Arif, J. S. Miller, *Inorg. Chem.* **2007**, *46*, 2471.

[16] A. E. Malkov, I. G. Fomina, A. A. Sidorov, G. G. Aleksandrov, I. M. Egorov, N. I. Latosh, O. N. Chupakhin, G. L. Rusinov, Yu. V. Rakitin, V. M. Novotortsev, V. N. Ikorskii, I. L. Eremenko, I. I. Moiseev, *J. Mol. Struct.* **2003**, *656*, 207 (CCDC Code: JOYPUI01).

[17] W. Libus, *Rocz. Chem.* **1962**, *36*, 999.

[18] J. S. Miller, *Angew. Chem.* **2006**, *118*, 2570; *Angew. Chem. Int. Ed.* **2006**, *45*, 2508.

[19] E. L. Pace, L. J. Noe, *J. Chem. Phys.* **1968**, *49*, 5317.

[20] A. T. Casey, S. Mitra in *Theory and Application of Molecular Paramagnetism*, (Eds.: E. A. Boudreaux, L. N. Mulay), Wiley, New York, **1976**; in this book the reported range for high-spin Fe^{II} is $3.37 \leq \chi T \leq 3.85$ (p. 200); for Mn^{II} $3.25 \leq \chi T \leq 4.41$ (p. 185); for Co^{II} $2.42 \leq \chi T \leq 3.39$ emu K/mol (p. 214).

[21] E. Sryjewski, N. Giordano, *Adv. Phys.* **1977**, *26*, 487.

[22] A. B. P. Lever in *Inorganic Electronic Spectroscopy*, Elsevier, Amsterdam, Oxford, New-York, Tokyo, **1984**, p. 461.

[23] Ø. Hatlevik, A. M. Arif, J. S. Miller, *J. Phys. Chem. Solids* **2004**, *65*, 61.

[24] J. V. Quagliano, A. K. Banerjee, V. L. Goedken, L. M. Vallarino, *J. Am. Chem. Soc.* **1970**, *92*, 482.

[25] W. E. Buschmann, J. S. Miller, *Chem. Eur. J.* **1998**, *4*, 1731.

[26] K. L. Rollick, J. K. Kochi, *Organometallics* **1982**, *1*, 725. Our data for the Fe^{III}/Fe^{II} couple is 0.11 eV higher than that reported in this reference, most probably, due to reference electrode and measurement temperature differences.

[27] K. Kirchner, R. Jedlicka, R. Schmid, *Monatsh. Chem.* **1982**, *123*, 203. R. Schmid, K. Kirchner, F. L. Dickert, *Inorg. Chem.* **1988**, *27*, 1530.

[28] a) S. Bhaduri, A. J. Tasiopoulos, M. A. Bolcar, K. A. Abboud, W. E. Streib, G. Christou, *Inorg. Chem.* **2003**, *42*, 1483; b) D. Harris, *Quantitative Chemical Analysis*, 4th ed., Freeman, New York, **1995**, p. AP36; c) D. Harris, *Quantitative Chemical Analysis*, 4th ed., Freeman, New York, **1995**, p. AP34.

[29] D. A. Dixon, J. S. Miller, *J. Am. Chem. Soc.* **1987**, *109*, 3656.

[30] T. B. Swanson, V. W. Laurie, *J. Phys. Chem.* **1965**, *69*, 244.

[31] W. E. Buschmann, J. S. Miller, *Chem. Eur. J.* **1998**, *4*, 1731.

[32] K. F. Purcell, J. C. Kotz, *Inorganic Chemistry*, Saunders, Philadelphia, **1977**, p. 235, and references therein.

[33] A. B. Pangborn, M. A. Giardello, R. H. Grubbs, R. K. Rosen, F. J. Timmers, *Organometallics* **1996**, *15*, 1518.

[34] A. Altomare, M. C. Burla, M. Camalli, G. Cascarano, C. Giacovazzo, A. Guagliardi, A. G. G. Moliteni, G. Polidori, R. Spagna, SIR97 (Release 1.02)—A program for automatic solution and refinement of crystal structure (*J. Appl. Cryst.* **1999**, *32*, 115–119).

[35] G. M. Sheldrick, SHELX97 (Includes SHELXS97, SHELXL97, CIFTAB), Programs for Crystal Structure Analysis (Release 97–2), University of Göttingen (Germany), **1997**.

[36] E. J. Brandon, D. K. Rittenberg, A. M. Arif, J. S. Miller, *Inorg. Chem.* **1998**, *37*, 3376.

Received: April 13, 2007